CARD8 inflammasome activation during HIV-1 cell-to-cell transmission

Jessie Kulsuptrakul[1,2], Michael Emerman[2,*], Patrick S. Mitchell[3,4*]
[1]Molecular and Cellular Biology Graduate Program, University of Washington, Seattle, WA 98195, USA

[2]Divisions of Human Biology and Basic Sciences, Fred Hutchinson Cancer Center, Seattle, WA 98109, USA

[3]Department of Microbiology, University of Washington, Seattle, WA 98109, USA

[4]Howard Hughes Medical Institute, University of Washington, Seattle, WA, 98109, USA

***Corresponding authors:** memerman@fredhutch.org, psmitche@uw.edu

Abstract

Our previous work demonstrated that CARD8 detects HIV-1 infection by sensing the enzymatic activity of the HIV protease, resulting in CARD8-dependent inflammasome activation (Kulsuptrakul et al., 2023). CARD8 recognition of HIV-1 protease activity is conferred by a HIV protease substrate mimic within the CARD8 N-terminus, which when cleaved by HIV protease triggers CARD8 inflammasome activation. Here, we sought to understand CARD8 responses to HIV-1 when the virus is transmitted through cell-to-cell infection from infected cells to target cells via a viral synapse. We observed that cell-to-cell transmission of HIV-1 induces CARD8 inflammasome activation in immortalized cells and primary human monocyte-derived macrophages in a manner that is dependent on viral protease activity and largely independent of the NLRP3 inflammasome. Additionally, to further evaluate the viral determinants of CARD8 sensing, we tested a panel of HIV protease inhibitor resistant clones to establish how variation in HIV protease affects CARD8 activation. We identified mutant HIV-1 proteases that differentially cleave and activate CARD8 compared to wildtype HIV-1, thus indicating that natural variation in HIV protease affects not only the cleavage of the viral Gag-Pol polyprotein but also likely impacts innate sensing and inflammation.

33 **INTRODUCTION**

34 HIV-1 disease progression is characterized by chronic inflammation, immune activation,
35 CD4+ T cell depletion and eventual destruction of the immune system and susceptibility to
36 opportunistic infections. The primary cellular targets of HIV-1 are activated CD4+ T helper cells,
37 specialized CD4+ T cell subtypes such as Th17 cells (Brenchley et al., 2008; Gosselin et al.,
38 2009; Rodriguez-Garcia et al., 2014), central memory cells (Chun et al., 1997b, 1997a, 1995),
39 and macrophages (Collman et al., 1990, 1989). Chronic immune activation is primarily caused
40 by rapid depletion of mucosal Th17 cells responsible for maintaining gut epithelial barrier
41 integrity (Brenchley et al., 2008, 2006). In addition to inflammation induced by circulating
42 microbial ligands, inflammation can also originate from HIV-infected cells through activation of
43 innate immune sensors that form cytosolic immune complexes known as inflammasomes.
44 Inflammasome activation ultimately results in activation of pro-inflammatory caspase 1
45 (CASP1), processing of inflammatory cytokines, and activation of a pore-forming protein
46 belonging to the gasdermin superfamily called gasdermin D (GSDMD), which forms small pores
47 in the cell membrane and initiates a lytic form of cell death known as pyroptosis, releasing
48 mature inflammatory cytokines interleukin (IL)-1β and IL-18 (Broz and Dixit, 2016; Fink and
49 Cookson, 2005).

50 In prior work, we and others showed that the inflammasome-forming sensor CARD8
51 senses HIV-1 infection through the detection of HIV-1 protease (HIV^{PR}) activity (Clark et al.,
52 2022; Kulsuptrakul et al., 2023; Wang et al., 2021). While the canonical function of HIV^{PR} is to
53 cleave viral polyproteins during virion maturation, active HIV^{PR} is also released into the host cell,
54 which is sensed by CARD8 via HIV^{PR} cleavage of its N-terminus and subsequent inflammasome
55 activation. In this way, the CARD8 N-terminus functions as a “molecular tripwire” to recognize
56 the enzymatic activity of HIV^{PR} and other viral proteases (Castro and Daugherty, 2023; Nadkarni
57 et al., 2022; Tsu et al., 2023). Moreover, HIV^{PR} cleavage of CARD8 occurs rapidly after infection
58 such that HIV^{PR} inhibitors and fusion inhibitors, but not reverse transcriptase inhibitors can

59 prevent CARD8 inflammasome activation, implying that CARD8 detects HIV-1 viral protease
60 activity of virion-packaged HIV^{PR} or "incoming" HIV^{PR} upon virion fusion (Kulsuptrakul et al.,
61 2023; Wang et al., 2024, 2021). Interestingly, CARD8 inflammasome activation in resting CD4+
62 T cells results in pyroptosis but not the release of pro-inflammatory cytokines IL-1β or IL-18
63 (Wang et al., 2024), suggesting that the activation of CARD8 in T cells does not directly
64 contribute to chronic inflammation. Here, we address whether or not CARD8 may influence HIV-
65 1 pathogenesis through the maturation and release of IL-1β from infected macrophages.
66 HIV-1 can be transmitted from one cell to another via two main mechanisms: "cell-free"
67 infection through binding of free HIV-1 virions to target cells, and cell-to-cell infection whereby
68 infected cells directly transfer virus to an uninfected target cell via the formation of a transient
69 viral synapse (Chen et al., 2007; Galloway et al., 2015; Iwami et al., 2015). Cell-to-cell
70 transmission of HIV-1 has been reported between multiple HIV-1 target cell types including
71 between active and resting CD4+ T cells (Agosto et al., 2018; Martin et al., 2010) and between
72 CD4+ T cells and macrophages (Baxter et al., 2014; Dupont and Sattentau, 2020; Lopez et al.,
73 2019). Cell-to-cell transmission delivers a large influx of virus to target cells, resulting in a high
74 multiplicity of infection (MOI) (Agosto et al., 2015; Del Portillo et al., 2011; Duncan et al., 2013;
75 Russell et al., 2013), which has been proposed to enhance viral fitness by overwhelming host
76 restriction factors including Tetherin/BST-2 (Jolly et al., 2010; Zhong et al., 2013), SAMHD1 (Xie
77 et al., 2019), and TRIM5α (Richardson et al., 2008), evading adaptive immune responses
78 including broadly neutralizing antibodies (Abela et al., 2012; Dufloo et al., 2018). Cell-to-cell
79 spread of HIV-1 is thus an important consideration in studying CARD8 inflammasome activation.
80 Here, we investigate both host and viral determinants of CARD8 inflammasome
81 activation upon HIV-1 infection. We evaluate CARD8 sensing of HIV^{PR} during cell-to-cell
82 transmission of HIV-1 to myeloid cells and find that CARD8 inflammasome activation occurs in
83 the context of cell-to-cell transmission to both THP-1 cells, an acute myeloid leukemia cell line,
84 and in primary monocyte-derived macrophages. Our findings suggest that CARD8 sensing of

85 HIV^{PR} during cell-to-cell transmission of HIV-1 to macrophages may be a source of inflammatory
86 cytokines that promote pathogenic chronic inflammation and disease progression. In addition,
87 we also show that natural variation in HIV^{PR} due to resistance to protease inhibitors also affects
88 CARD8 cleavage and subsequent inflammasome activation. Our results extend the role of
89 incoming HIV^{PR} on CARD8-dependent activation of inflammasome responses as a function of
90 cell type, mode of transmission, and virus evolution in response to antiviral therapy.
91
92
93 **RESULTS**

94 ***Cell-to-cell transmission of HIV-1 induces CARD8 inflammasome activation***

95 Our previous work investigating HIV-dependent CARD8 inflammasome activation used
96 the cationic polymer DEAE-dextran, which is a common reagent to enhance viral infection in cell
97 culture (Bailey et al., 1984). However, we occasionally found that DEAE-dextran could induce
98 inflammasome activation in the absence of viral infection. To formally evaluate this, we first
99 assessed whether or not we could observe CARD8-dependent inflammasome activation in a
100 cell-free infection system in the absence of DEAE-dextran. We infected either wildtype (WT) or
101 *CARD8* knockout (KO) THP-1 cells with HIV-1_{LAI} in either the presence or absence of DEAE-
102 dextran and measured cell death and IL-1β secretion 24 hours post-infection as readouts of
103 inflammasome activation. We found that despite achieving similar levels of infection (20-30%)
104 as measured by intracellular p24^{gag} after spinoculation with and without DEAE-dextran (**Figure**
105 **1A, left**), we only detected robust CARD8-dependent inflammasome activation in WT THP-1
106 cells infected in the presence of DEAE-dextran (**Figure 1A,** middle and right). These data
107 suggest that cationic polymer is necessary to observe HIV-dependent CARD8 inflammasome
108 activation in our cell-free system.

109 These results prompted us to establish other models of HIV-1 infection and subsequent
110 inflammasome activation that lack cationic polymers. Thus, we designed an *in vitro* coculture

111 infection system to mimic HIV-1 cell-to-cell transmission by infecting SUPT1 cells, a T-cell
112 lymphoma line (i.e., donor cells) and then mixing them with uninfected THP-1 cells (i.e., target
113 cells). We opted for SUPT1 cells as the viral producer cell line because they are permissive to
114 HIV-1 infection, and unlike THP-1 cells, SUPT1 cells do not respond to a known CARD8
115 inflammasome activator, ValboroPro (VbP), as assayed by both IL-1β secretion and cell death,
116 indicating that SUPT1 cells do not have a functional CARD8 inflammasome pathway (**Figure**
117 **1B, Figure 1-figure supplement 1A**). This allowed us to infer that inflammasome outputs (i.e.
118 IL-1β secretion) in our coculture system occur upon cell-to-cell transmission of HIV-1 from
119 SUPT1 cells to the CARD8-competent THP-1 cells.

120 We found that coculture of THP-1 cells with HIV-1_{LAI}-infected but not mock-infected
121 SUPT1 cells results in robust inflammasome activation as indicated by IL-1β secretion,
122 suggesting that our coculture system, which lacks DEAE-dextran, can induce HIV-dependent
123 inflammasome activation via cell-to-cell infection (**Figure 1D**). To further test this assumption,
124 we prevented cell-to-cell contact using a virus-permeable transwell with a 0.4μm pore insert
125 (**Figure 1C**). In contrast to the cell-to-cell condition, HIV-1_{LAI}-infected SUPT1 cells (upper
126 chamber) co-cultured with THP-1 cells (bottom chamber) did not lead to detectable IL-1β
127 secretion (**Figure 1D**) despite equivalent amounts of free infectious virus as measured by
128 reverse transcriptase level in the supernatant from the lower chamber **(Figure 1-figure**
129 **supplement 1B**). However, transmission of HIV-1 through the transwell from infected SUPT1
130 cells to THP-1 cells and subsequent inflammasome activation was observed when media was
131 supplemented with DEAE-dextran (**Figure 1D**), indicating that in the absence of cationic
132 polymer, inflammasome activation in our SUPT1:THP-1 coculture system is triggered following
133 HIV-1 cell-to-cell transmission.

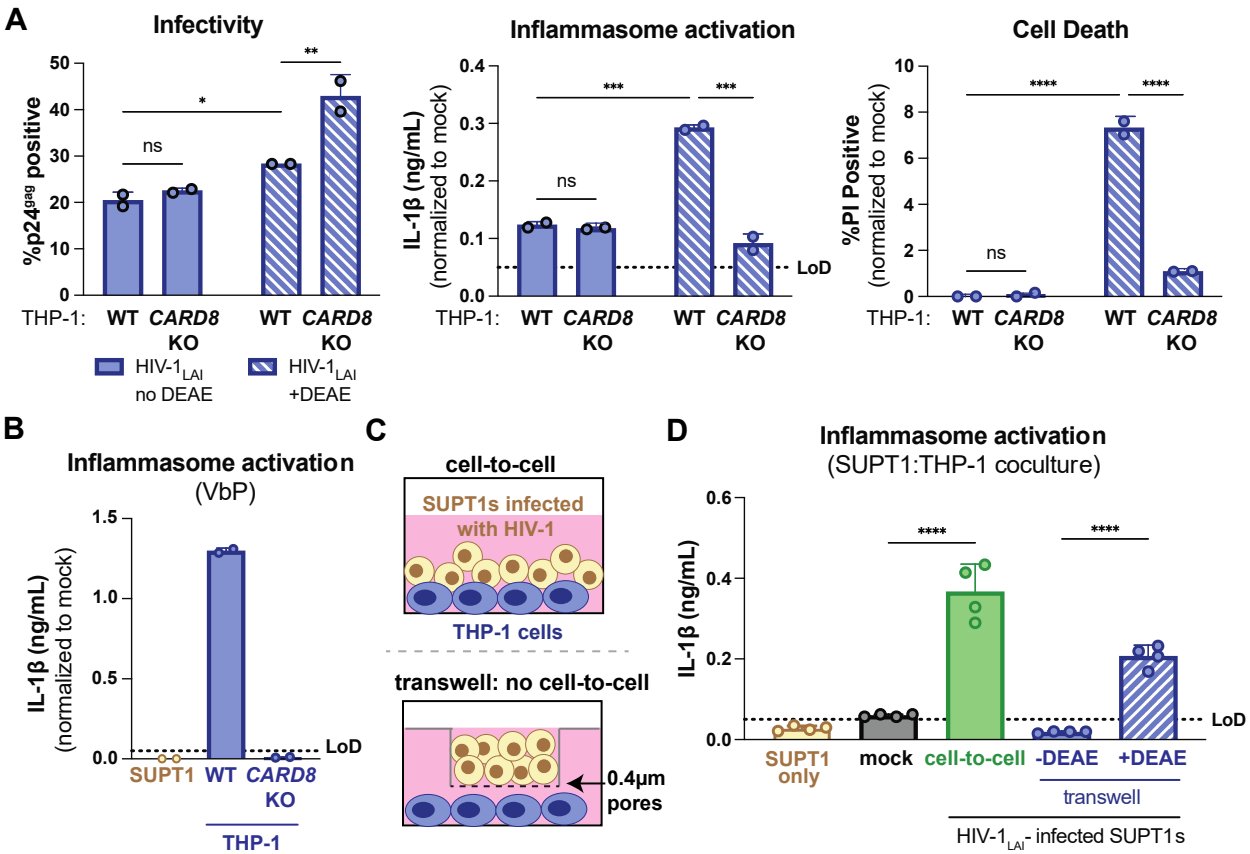

Figure 1. HIV-1 cell-to-cell infection induces inflammasome activation. (**A**) Wildtype (WT) or *CARD8* knockout (KO) THP-1 cells were infected with HIV-1_{LAI} at the same MOI in the presence or absence of DEAE-dextran (10µg/mL) then harvested after 24 hours and assayed for: left) percent infection via intracellular $p24^{gag}$, middle) inflammasome activation by IL-1β secretion via IL-1R reporter assay, and right) cell death via propidium iodide (PI) dye uptake using flow cytometry. (**B**) SUPT1 or THP-1 cells were primed with Pam3CSK4 (500ng/mL) overnight then treated with 5µM ValboroPro (VbP) for 24 hours then assessed for IL-1β secretion as in (A). (**C**) Schematic illustrating experimental setup for SUPT1:THP-1 cell coculture. (**D**) THP-1 cells were primed overnight with Pam3CSK4 prior to coculture. SUPT1 cell were either mock infected or infected with HIV-1_{LAI} then cocultured with primed WT THP-1 cells 20 hours post infection. Mock- or HIV-1_{LAI}-infected SUPT1 cells were either mixed with the THP-1 cells or put in a transwell with a virus-permeable membrane in the presence or absence of DEAE-dextran. DEAE-dextran was added to the mock but not the mixed condition. Supernatant from the cocultures were harvested 3 days after starting the coculture and assayed for IL-1β secretion as in A) and B). Dotted line indicates limit of detection (LoD). Datasets represent mean ± SD (A-B: n=2; D n=4 biological replicates). A-B: Two-way ANOVA with Tukey's test D: One-way ANOVA with Tukey's test using GraphPad Prism 10. ns = not significant, *p<0.05,**p<0.01, ***p<0.001, ****p<0.0001.

154

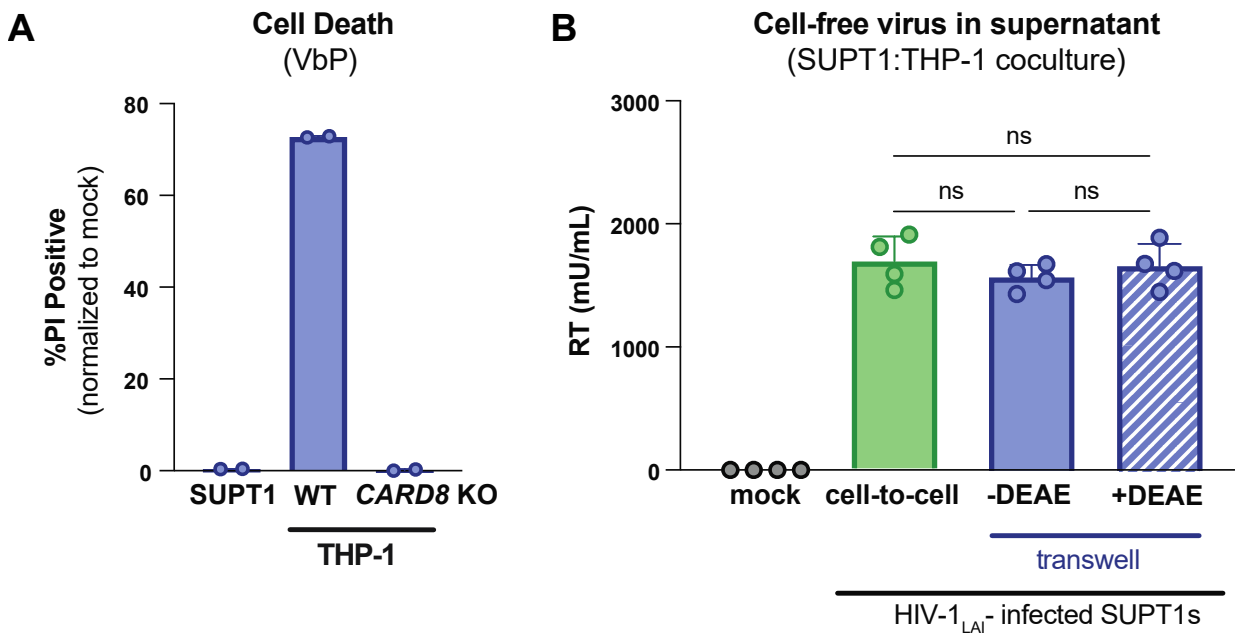

155

156 **Figure 1- figure supplement 1. HIV-1 cell-to-cell infection induces inflammasome**
157 **activation.** (A) SUPT1 or THP-1 cells were primed with Pam3CSK4 (500ng/mL) overnight then
158 treated with 5μM ValboroPro (VbP) for 24 hours then assessed for cell death via propidium
159 iodide (PI) uptake. (B) SUPT1 cells were cocultured with THP-1 cells as in Figure 1D and
160 supernatant in the cell-to-cell condition and in the supernatant outside of the transwell was
161 sampled and measured for cell-free infectious HIV virions via reverse transcriptase (RT) assay.
162 Datasets represent mean ± SD (A: n=2; B: n=4 biological replicates). B: Two-way ANOVA with
163 Tukey's test using GraphPad Prism 10. ns = not significant

164 We next assessed the role of CARD8 and other inflammasome sensors during cell-to-
165 cell transmission of HIV-1. We cocultured mock- or HIV-1_{LAI}-infected SUPT1 cells with either WT
166 or *CARD8* KO THP-1 cells and compared inflammasome activation by measuring levels of
167 secreted IL-1β. HIV-1_{LAI}-infected SUPT1 cells cocultured with WT but not *CARD8* KO THP-1
168 cells resulted in a significant increase in IL-1β (**Figure 2A**). These results suggest that CARD8
169 is the primary sensor that drives inflammasome activation in HIV-1 cell-to-cell transmission to
170 THP-1 cells. Since the NLRP3 inflammasome has previously been implicated in HIV-dependent
171 inflammasome activation in CD4+ T cells (Zhang et al., 2021), we also assessed the effects of
172 the NLRP3 inflammasome-specific inhibitor MCC950 (Coll et al., 2015; Primiano et al., 2016) on
173 inflammasome activation in our coculture system. Treatment with MCC950 or the CASP1

174 inhibitor VX765 (Wannamaker et al., 2007) were sufficient to abrogate inflammasome activation
175 induced by the ionophore nigericin, a well-characterized NLRP3 agonist (**Figure 2- figure**
176 **supplement 1A**). However, in the HIV-1 coculture system, MCC950 treatment had only a
177 modest effect on inflammasome activation while VX765 and the HIV^{PR} inhibitor lopinavir (LPV),
178 which prevents CARD8 cleavage by HIV-1^{PR} (Kulsuptrakul et al., 2023; Wang et al., 2021),
179 completely abrogated IL-1β secretion (**Figure 2B**). We observed similar results during cell-free
180 infection of THP-1 cells in the presence of DEAE-dextran (**Figure 2- figure supplement 1B**).
181 Taken together, these findings indicate that HIV-dependent inflammasome activation is CARD8-
182 dependent and largely NLRP3-independent.

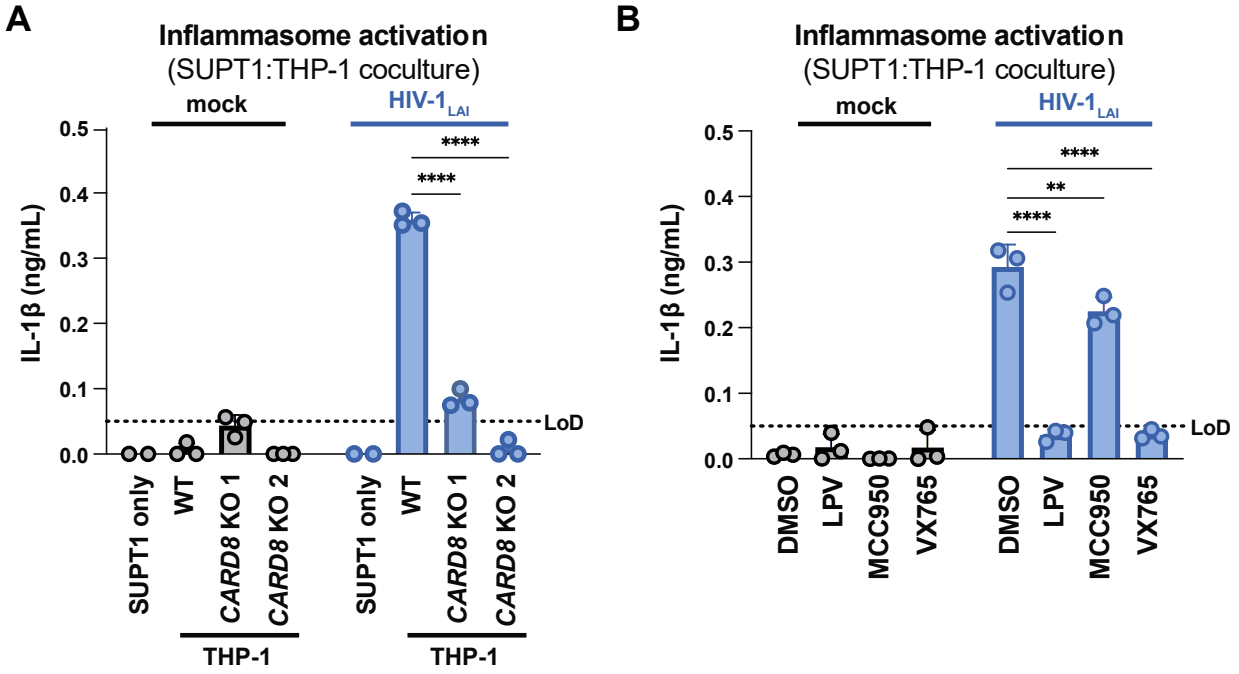

183

184 **Figure 2. HIV-1 cell-to-cell transmission induces CARD8-dependent activation largely**
185 **independent of NLRP3.** (**A**) SUPT1 cells were either mock-infected or infected with HIV-1$_{LAI}$ for
186 18-20 hours prior to coculture with wildtype (WT) or *CARD8* knockout (KO) THP-1 cells. The
187 coculture was harvested 72 hours later to probe for IL-1β secretion in the coculture supernatant
188 via IL-1R reporter assay. THP-1 cells were primed with Pam3CSK4 (500ng/mL) for 16-24 hours
189 prior to coculture. SUPT1 cells were infected with HIV-1$_{LAI}$ such that 30% of the cells were
190 positive for intracellular p24^{gag} after 18-20 hours. (**B**) SUPT1 cells were either mock or HIV-1$_{LAI}$-
191 infected as in (A) for 18-20 hours then incubated in DMSO, lopinavir (LPV), MCC950, or VX765
192 at 0.01%, 5μM, 10μM, or 1μg/mL, respectively, for 15 minutes prior to coculturing with primed
193 WT THP-1 cells. The coculture was assessed for subsequent inflammasome activation after 72

194 hours as in (A). Dotted line indicates limit of detection (LoD). Datasets represent mean ± SD
195 (n=3 biological replicates). Two-way ANOVA with Dunnett's test using GraphPad Prism 10. ns =
196 not significant, *p<0.05,**p<0.01, ***p<0.001, ****p<0.0001.
197

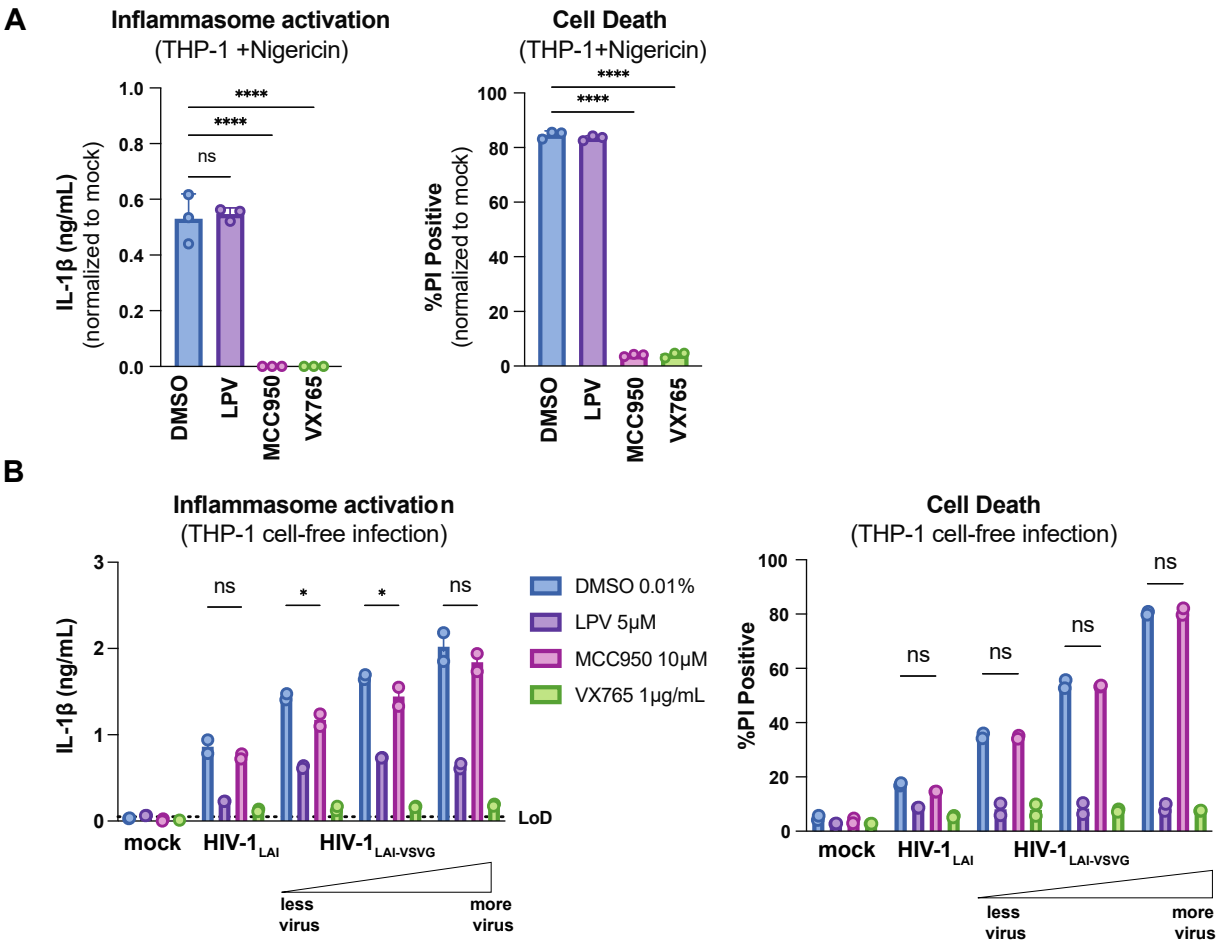

198

199 **Figure 2- figure supplement 1. HIV-dependent inflammasome activation is largely NLRP3-**
200 **independent.** (**A**) Wildtype THP-1 cells were pre-treated with either DMSO, lopinavir (LPV),
201 MCC950, or VX765 at 0.01%, 5μM, 10μM, or 1μg/mL, respectively, for 15 minutes prior to 4-
202 hour treatment with 5μg/mL nigericin. Subsequent inflammasome activation was assessed via
203 (A-left) IL-1β secretion via IL-1R reporter assay and (A-right) cell death via propidium iodide (PI)
204 dye uptake. (**B**) Wildtype THP-1 cells were pre-treated with indicated inhibitors as in (A) then
205 infected with either HIV-1_{LAI} or increasing amounts of VSV-G pseudotyped HIV-1_{LAI} (HIV-1_{LAI-}
206 $_{VSVG}$) in the presence of 10μg/mL DEAE-dextran. Subsequent inflammasome activation was
207 assessed 24 hours post infection via IL-1β secretion and cell death as in (A). Dotted line
208 indicates limit of detection (LoD). Datasets represent mean ± SD (A: n=3, B: n=2 biological
209 replicates). One-way (A) or Two-way (B) ANOVA with Dunnett's test using GraphPad Prism 10.
210 ns = not significant, *p<0.05,**p<0.01, ***p<0.001, ****p<0.0001.
211

212 **CARD8 is required for inflammasome activation during HIV-1 cell-to-cell transmission**
213 **into primary monocyte-derived macrophages**

214 We next examined inflammasome activation upon HIV-1 cell-to-cell transmission in
215 primary human monocyte-derived macrophages (MDMs). Previously, we had observed that
216 CARD8 could sense active HIV-1^{PR} released into the host cytosol following viral fusion, which
217 we refer to as "incoming" HIV-1^{PR} in our cell-free infection system in THP-1 cells using DEAE-
218 dextran and spinoculation (Kulsuptrakul et al., 2023). Thus, we assessed the importance of viral
219 entry by coculturing MDMs from three independent healthy donors with mock-, HIV-1$_{LAI}$-, or HIV-
220 1$_{NL4.3-BaL}$-infected SUPT1 cells expressing CCR5 (SUPT1-CCR5) and assayed for
221 inflammasome activation (**Figure 3A**). HIV-1$_{LAI}$ is a CXCR4 tropic strain unable to infect
222 macrophages whereas HIV-1$_{NL4.3-BaL}$ is a CCR5 and macrophage-tropic strain. We observed
223 inflammasome activation, as measured by IL-1β secretion, in MDMs cocultured with HIV-1$_{NL4.3-}$
224 $_{BaL}$-infected SUPT1 cells but not in MDMs cocultured with mock- or HIV-1$_{LAI}$-infected SUPT1-
225 CCR5 cells (**Figure 3A**). This demonstrates that HIV-dependent inflammasome activation can
226 occur in MDMs during cell-to-cell infection in a manner dependent on viral entry. To further
227 ascertain if this activation was CARD8-dependent and driven by incoming HIV^{PR} during
228 SUPT1:MDM cell-to-cell transmission, we investigated the effects of different inhibitors on
229 activation in MDM cocultures with HIV-1$_{NL4.3-BaL}$-infected SUPT1s. We observed that IL-1β
230 secretion was abrogated by treatment with lopinavir and VX765, indicating that inflammasome
231 activation in MDM cocultures is dependent on HIV^{PR} and CASP1, respectively (**Figure 3A**). In
232 addition, we used a reverse transcriptase inhibitor, nevirapine (NVP), to prevent synthesis of *de*
233 *novo* translated HIV^{PR}, and thus any CARD8-dependent IL-1β secretion would only be due to
234 incoming HIV^{PR} in the presence of NVP. Indeed, we observed HIV-dependent inflammasome
235 activation in the presence of NVP treatment that was added at the time of co-culture, indicating
236 that incoming HIV^{PR} is sufficient to elicit an inflammasome response (**Figure 3A**). Lastly, MDM
237 cocultures treated with MCC950, an inhibitor of the NLRP3 inflammasome, had no effect on IL-

238 1β secretion (**Figure 3A**). Thus, cell-to-cell contact of infected cells with primary monocyte-
239 derived macrophages can elicit an inflammasome response in a manner that is dependent on
240 viral entry, CASP1, and incoming HIV^{PR}, and independent from NLRP3. Taken together, these
241 data suggest that in the context of cell-to-cell transmission, CARD8 is likely the inflammasome-
242 forming sensor that detects HIV-1 infection via incoming HIV^{PR} activity in primary macrophages.
243 To more definitively probe the role of CARD8 in HIV-1 induced inflammasome activation
244 in MDMs, we genetically edited MDMs by isolating monocytes from three healthy donors and
245 electroporating them with Cas9 RNPs complexed with three unique sgRNAs per gene targeting
246 either *AAVS1*, a safe harbor locus, or *CARD8.* Edited MDMs were then differentiated for 6 days
247 prior to evaluating KO efficiency and initiating cocultures with HIV-1-infected SUPT1 cells. In all
248 three donors, we observed a marked reduction of the full-length and FIIND-processed CARD8
249 protein by immunoblotting with an antibody that detects the CARD8 C-terminus in *CARD8* KO
250 MDMs relative to the *AAVS1* KO control (**Figure 3B**). In addition, we confirmed both *CARD8*
251 and *AAVS1* KO at the genetic level via Synthego ICE analysis (Conant et al., 2022), measuring
252 >85% KO efficiency (**Figure 3B**). We also observed robust inflammasome activation upon
253 treatment with CARD8 inflammasome activator VbP as measured by IL-1β secretion in *AAVS1*
254 KO MDMs from 2 of the 3 donors, which was completely abrogated in *CARD8* KO MDMs,
255 confirming functional loss of CARD8 (**Figure 3C**). We next cocultured either *AAVS1* KO or
256 *CARD8* KO MDMs with mock or HIV-$1_{NL4.3\text{-}BaL}$-infected SUPT1-CCR5 cells at a 1:1 ratio and
257 measured inflammasome activation via IL-1β secretion 48 hours post-coculture. In all 3 donors,
258 we observed significant reduction in inflammasome activation in *CARD8* KO cocultures relative
259 to the *AAVS1* KO control (**Figure 3D**). Taken together, these data demonstrate that CARD8 is
260 required for inflammasome activation in MDMs during HIV-1 cell-to cell transmission.

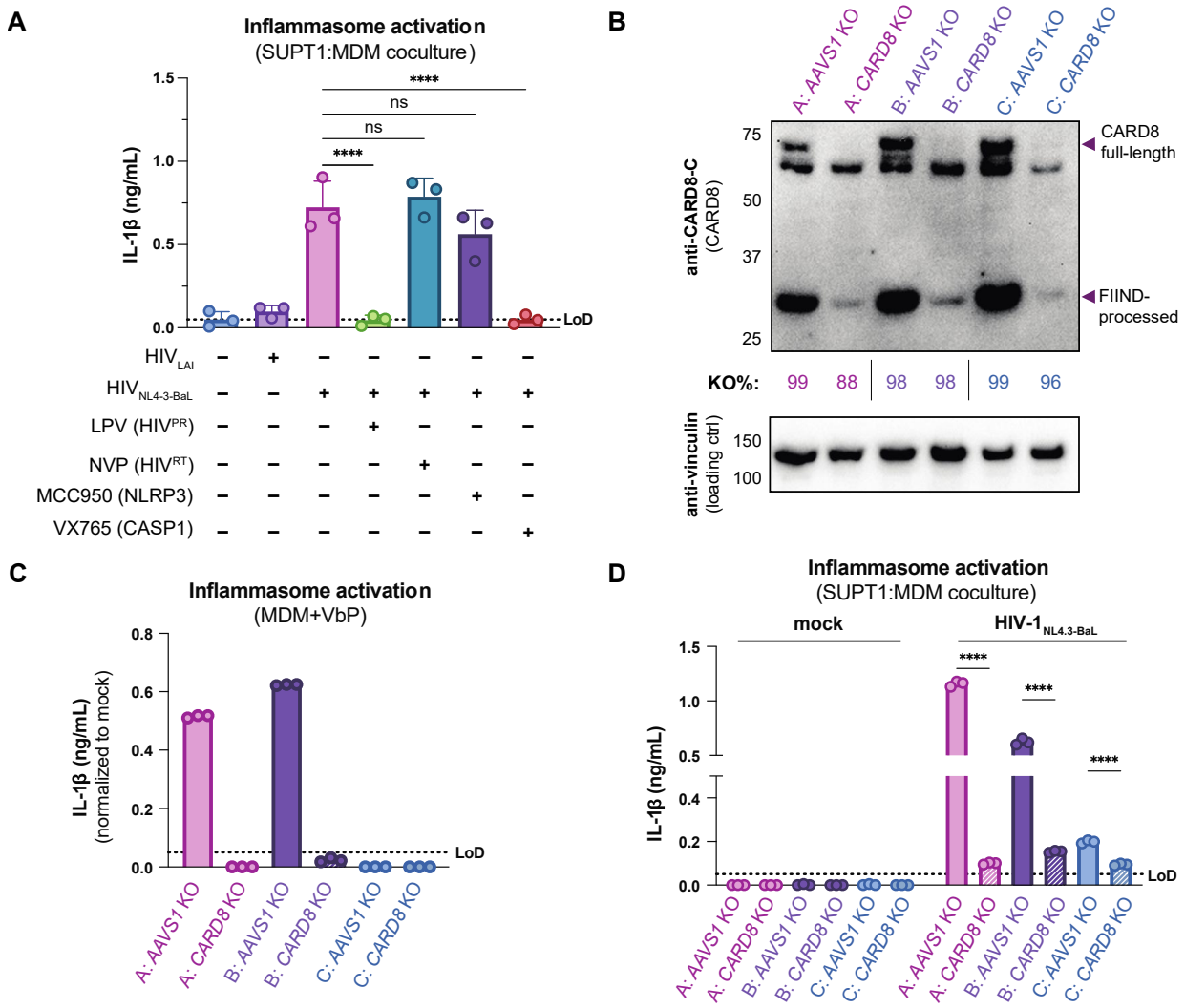

Figure 3. Cell-to-cell HIV infection induces CARD8-dependent activation in monocyte-derived macrophages (MDMs). (**A**) MDMs were cocultured with SUPT1 cells expressing CCR5 (SUPT1-CCR5) that were mock-, HIV-1_{LAI}- or HIV-$1_{NL4.3-BaL}$-infected then assayed for inflammasome activation 48 hours post-coculture for IL-1β secretion. Fifteen minutes before starting the coculture, SUPT1-CCR5 cells infected with HIV-$1_{NL4.3-BaL}$ were pre-treated with either DMSO, lopinavir (5μM), nevirapine (50μM), MCC950 (10μM) or VX765 (1μg/mL), inhibiting HIV-1 protease (HIV^{PR}), HIV-1 reverse transcriptase (HIV^{RT}), NLRP3, or caspase 1 (CASP1), respectively. SUPT1-CCR5 cells were infected with HIV-1_{LAI} and HIV-$1_{NL4.3-BaL}$ such that 2% and 7% of cells, respectively, were positive for intracellular $p24^{gag}$ after 24 hours. (**B**) MDMs from 3 independent healthy donors were knocked out (KO) for either *AAVS1* or *CARD8* using a Synthego gene KO kit and were immunoblotted using an anti-CARD8 antibody or anti-vinculin. Full-length and FIIND-processed CARD8 intermediates are marked with a purple arrow. Table between CARD8 and vinculin blot shows Synthego gene KO% scores for each

276 donor KO line. (**C**) *AAVS1* and *CARD8* KO MDM lines were primed with Pam3CSK4
277 (500ng/mL) overnight and then treated with ValboroPro (VbP) for 24 hours before assessing for
278 IL-1β secretion. (**D**) *AAVS1* and *CARD8* KO MDM lines were cocultured with SUPT1-CCR5
279 cells mock-, or HIV-$1_{NL4.3-BaL}$-infected then assayed for inflammasome activation 48 hours post-
280 coculture for IL-1β secretion. Dotted line indicates limit of detection (LoD). Datasets represent
281 mean ± SD (A: n=3 independent donors, C-D: n=3 technical replicates per donor). (A) One-way
282 or (D) two-way ANOVA with Tukey's test (using GraphPad Prism 10. ns = not significant,
283 *p<0.05,**p<0.01, ***p<0.001, ****p<0.0001.
284

285 ***Protease inhibitor resistant strains of HIV-1 differentially cleave and activate CARD8***

286 The consequences of CARD8 inflammasome activation on viral replication have been
287 challenging to assess given that viral fitness is intrinsically linked to viral protease processing of
288 the viral polyprotein such that inhibiting HIV^{PR} also prevents viral replication. In an attempt to
289 circumvent this issue, we surveyed a panel of multi-HIV^{PR} inhibitor-resistant (PI-R) infectious
290 molecular clones of HIV-1 (Varghese et al., 2013). This panel of PI-R molecular clones vary in
291 resistance to HIV protease inhibitors including nelfinavir (NFV), fosamprenavir (FPV), saquinavir
292 (SQV), indinavir (IDV), atazanavir (ATV), lopinavir (LPV), tipranavir (TPV), and darunavir (DRV).
293 Each molecular clone encodes 4 to 11 mutations in HIV^{PR} as well as various compensatory
294 HIV^{gag} mutations (Varghese et al., 2013) (**Table S1**).

295 We initially tested if PI-R HIV-1 proviruses differentially cleave CARD8 by co-transfecting
296 HEK293T cells with an expression plasmid encoding an N-terminal mCherry tagged human
297 CARD8 and either wildtype HIV-1_{LAI} or PI-R HIV-1 proviruses. HIV-1_{LAI} protease cleaves CARD8
298 between phenylalanine (F) 59 and F60 (Wang et al 2021), resulting in a ~33kDa product
299 (**Figure 4A-top**). By quantifying the 33kDa CARD8 cleavage product with each HIV-1 provirus,
300 we identified a PI-R clone that exhibited similar efficiency at cleaving CARD8 to HIV-1_{LAI} (i.e., PI-
301 R1), PI-R clones that were markedly less efficient at cleaving CARD8 than HIV-1_{LAI} (i.e., PI-R2,
302 PI-R3, PI-R5, PI-R9, and PI-R10) and two PI-R clones, PI-R12 and PI-R13, that were more
303 efficient at cleaving CARD8 than HIV-1_{LAI} (**Figure 4A-top, Table S1**). Of note, all PI-R
304 proviruses had similar levels of HIV^{PR} activity for HIV^{gagpol} polyprotein processing from $p55^{gag}$ to

305 $p24^{gag}$ as indicated by the ratio of $p24^{gag}/p55^{gag}$ quantified from the anti-$p24^{gag}$ immunoblot
306 (**Figure 4A-middle**). These results indicate that naturally occurring HIV-1 protease mutations
307 can influence host targets like CARD8.

308 We next assessed if PI-R clones exhibiting reduced (PI-R2 and -9) or increased (PI-R12
309 and -13) cleavage of CARD8 relative to HIV-1_{LAI} (**Figure 4A**, **4B**, and **Table S1**) resulted in
310 differential inflammasome activation. HEK293T cells endogenously express CARD8 but lack the
311 downstream components (i.e., CASP1, GSDMD, and IL-1β/IL18) of the inflammasome pathway.
312 Thus, we reconstituted the inflammasome pathway in HEK293T cells by co-transfection of
313 human caspase 1, human pro-IL-1β, and either empty vector, HIV-1_{LAI} or representative PI-R
314 proviruses then quantified CASP1-dependent processing of pro-IL-1β as a readout of CARD8
315 inflammasome activation as in (Tsu et al., 2023). Consistent with the observed differences in
316 CARD8 cleavage by PI-R clones (**Figure 4A**), we found that PI-R2 and PI-R9, which exhibited
317 less CARD8 cleavage than HIV-1_{LAI}, also induced lower IL-1β levels than HIV-1_{LAI} (**Figure 4B**).
318 Similarly, PI-R12 and PI-R13, which demonstrated enhanced CARD8 cleavage, elicited higher
319 IL-1β levels than HIV-1_{LAI} (**Figure 4B**). We next assessed inflammasome activation by the PI-R
320 clones in a cell-to-cell transmission model using HEK293T cells as donor cells rather than
321 SUPT1 cells and either WT or *CARD8* KO THP-1 cells as the target line at a 1:1 ratio. We opted
322 to overexpress the HIV-1_{LAI} or the PI-R proviruses in HEK293T cells rather than infecting
323 SUPT1 cells due to dramatic variability in replication kinetics between PI-R strains. In these
324 HEK293T:THP-1 cocultures, we observed that cell-to-cell transmission of PI-R2 and PI-R9
325 resulted in lower IL-1β levels while PI-R12 and PI-R13 resulted in higher IL-1β levels compared
326 to HIV-1_{LAI}, respectively (**Figure 4C**), consistent with our findings from CARD8 cleavage (**Figure**
327 **4A**) and reconstituted inflammasome assays (**Figure 4B**). Our findings suggest that HIV-
328 dependent inflammasome activation is under genetic control of the viral protease in a manner
329 that can be increased or decreased with naturally occurring mutations induced by drug
330 resistance.

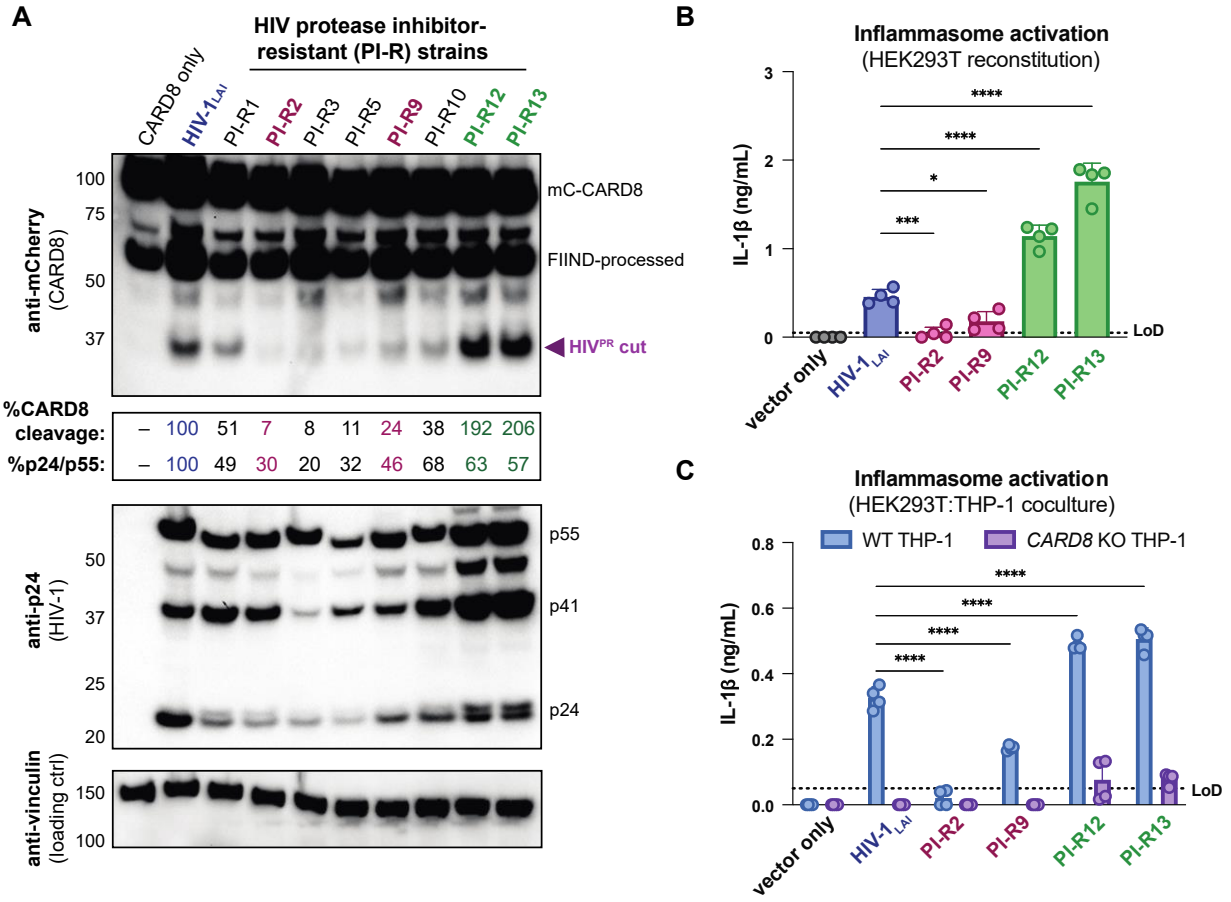

Figure 4. Protease inhibitor resistant strains of HIV-1 differentially cleave and activate CARD8. (**A**) HEK293T cells were transfected with a construct encoding CARD8 with an N-terminal mCherry tag (mCherry-CARD8) and indicated HIV-1 proviral constructs. Protease inhibitor-resistant (PI-R) clones of HIV-1 are a subset of a panel expressing prototypical multidrug resistant HIV-1 protease (HIV^{PR}) in an NL4.3 backbone (Table S1). Top: Immunoblotting using anti-mCherry antibody to detect mCherry-CARD8. The full-length (mc-CARD8) and FIIND-processed bands are indicated as well as the HIV^{PR} cut product. The band at ~45 kDa is the result of cleavage by the 20S proteasome. % CARD8 cleavage was calculated by quantifying the HIV^{PR} cut band relative to the HIV-1_{LAI} control using BioRad Image Lab 6. Middle: Immunoblotting with an anti-$p24^{gag}$ antibody showing HIV-1^{gag} cleavage products $p41^{gag}$ and $p24^{gag}$, and/or full-length HIV-1^{gag}, $p55^{gag}$. %p24/p55 was calculated from the ratio of $p24^{gag}$ versus $p55^{gag}$ product by quantifying the volume of the $p24^{gag}$ bands versus the $p55^{gag}$ band relative to the HIV-1_{LAI} control using BioRad Image lab 6. Bottom: Immunoblotting with an anti-vinculin antibody to detect vinculin as a loading control. (**B**) HEK293T cells were transfected with human caspase 1 and human pro-IL-1β, and either carrier vector or indicated HIV-1 proviruses then probed for IL-1β secretion 24 hours post-transfection via IL-1R reporter assay. (**C**) HEK293T cells were transfected with indicated HIV-1 proviruses (300ng). 24 hours post-transfection either wildtype (WT) or *CARD8* knockout (KO) THP-1s were overlayed on the transfected HEK293T cells in a 1:1 ratio. THP-1s were primed with Pam3CSK4 overnight prior

352 to coculture. Supernatants were harvested 24 hours post coculture to assay for IL-1β secretion
353 as in (B). Dotted line indicates limit of detection (LoD). Datasets represent mean ± SD (n=4
354 biological replicates). p-Values were determined by two-way ANOVA with Dunnett's test using
355 GraphPad Prism 10. ns = not significant, *p<0.05,**p<0.01, ***p<0.001, ****p<0.0001.
356

357 **Table S1: Protease inhibitor resistance mutations and relative CARD8 cleavage.**

Clone name	PI-resistance mutations in HIV^{PR}	HIV^{gag} mutation	Strongest PI-R[1]	% CARD8 cleavage (relative to HIV_{LAI})
$HIV\text{-}1_{LAI}$	wildtype	wildtype	wildtype	100
CA126802 (PI-R1)	11I, 32I, 33F, 46I, 47V, 54M, 58E, 73S, 84V, 89V, 90M	A431V (NC/p1) I437N (NC/p1) P453LF (p1/p6)	FPV, LPV, TPV, DRV	51
CA122805 (PI-R2)	**10F, 33F, 43T, 46L, 54V, 82A, 84V, 90M**	**A431V (NC/p1) R532S (p1/p6)**	**SQV**	**7**
CA126805 (PI-R3)	33F, 43T, 46I, 48V, 50V, 54S, 82A	I437N (NC/p1) L449VF (p1/p6) PTAP insertion (p6)	SQV, IDV, LPV	**8**
CA96457 (PI-R5)	48V, 53L, 54V, 82A, 90M	K436R (NC/p1)	SQV	11
CA96458 (PI-R9)	**10F, 30N, 33F, 43T, 84V, 88D, 90M**	**A431V (NC/p1)**	**NFV, SQV**	**24**
CA50834-1 (PI-R10)	24I, 46I, 54V, 76V, 82T	A431V (NC/p1)	IDV, LPV	38
CA96451 (PI-R12)	**32I, 33F, 43T, 46I, 47V, 54M, 73S, 82A, 89V, 90M**	**I437N (NC/p1) PTAP insertion (p6)**	**FPV, LPV**	**192**
CA20392-1 (PI-R13)	**24I, 46L, 54V, 82A**	**A431V (NC/p1)**	**LPV**	**206**

358 **Table S1** shows the protease inhibitor-resistant (PI-R) clones assayed in **Figure 4** with
359 corresponding mutations in HIV protease (HIV^{PR}) and HIV^{gag}. [1]These clones were previously
360 cloned and assayed for PI-R in (Varghese et al., 2013). The PI-R subset used in Figure 4B are
361 bolded and highlighted in red or green and denote either hypo- or hyper-active CARD8
362 cleavage, respectively. NFV-nelfinavir; FPV- fosamprenavir; SQV- saquinavir; IDV- indinavir;
363 LPV- lopinavir; TPV- tipranavir; DRV- darunavir. The consensus subtype B sequence can be
364 found on the Stanford HIV Drug Resistance Database (HIVDB) ("Stanford - HIV Drug
365 Resistance Database," n.d.). Relative CARD8 cleavage was determined by quantifying band
366 volume of the CARD8 cleavage product in BioRad Image Lab 6 and comparing to cleavage with
367 $HIV\text{-}1_{LAI}$.
368

369 **DISCUSSION**

370 We demonstrate that cell-to-cell transmission of HIV-1 to myeloid cells yields CARD8-
371 dependent inflammasome activation via incoming HIV^{PR}. This activation occurs in a largely
372 NLRP3-independent manner in these myeloid cell types despite being previously implicated as
373 an innate HIV sensor in CD4+ T cells (Zhang et al., 2021). In addition, we identified protease
374 inhibitor resistant strains of HIV-1 that differentially cleave and activate the CARD8
375 inflammasome. Thus, HIV^{PR} mutants selected for their resistance to different protease inhibitors
376 also affect their ability to cleave host proteins including the inflammasome-forming sensor
377 CARD8.

378

379 ***CARD8 as the primary innate sensor of HIV-1 infection***

380 Previously, both the NLRP3 and IFI16 inflammasomes have been implicated as innate
381 sensors of HIV-1 infection and drivers of CD4+ T cell depletion using blood and lymphoid-
382 derived CD4+ T cells, respectively, and cell-to-cell transmission was reported to be crucial for
383 IFI16 sensing of abortive HIV transcripts (Doitsh et al., 2014; Galloway et al., 2015; Monroe et
384 al., 2014; Zhang et al., 2021). However, the mechanism of activation of NLRP3 activation in
385 response to HIV-1 remains elusive. Similarly, there have been reports that IFI16 is not an
386 inflammasome-forming sensor, and instead a nuclear transcriptional regulator of antiviral genes
387 including type I interferons and RIG-I (Hornung et al., 2009; Jiang et al., 2021; Thompson et al.,
388 2014), suggesting that there may be other mechanisms of CD4+ T cell depletion and HIV-
389 dependent inflammasome activation at play. Indeed, CARD8, which is expressed and functional
390 in naïve and memory CD4+ and CD8+ T cells (Linder et al., 2020), was recently shown to be
391 required for pyroptosis in primary human blood- and lymphoid-derived CD4+ T cells and
392 humanized mouse models (Wang et al., 2024), implicating CARD8 as a major driver of CD4+ T
393 cell depletion during HIV-1 infection. In this study and our prior work (Kulsuptrakul et al., 2023),
394 we demonstrate that CARD8 is also the primary innate sensor during HIV-1 infection in myeloid

395 cell types. However, our present study does not rule out the possibility that under certain
396 conditions or in certain cell types, NLRP3 activation may occur, for example following GSDMD
397 pore formation following CARD8 inflammasome activation and play a more profound role in
398 promoting HIV-dependent inflammation. Nonetheless, these data along with other recent work
399 (Wang et al., 2024) strongly suggest that CARD8 is a major innate sensor of HIV-1 infection.
400

401 ***Protease inhibitor resistance mutations and inflammatory disease***

402 Given the important role of HIV^{PR} in replication, early combination antiretroviral therapy for
403 people living with HIV (PLWH) included protease inhibitors along with reverse transcriptase
404 inhibitors. However, resistance mutations to protease inhibitors quickly arose in PLWH through
405 mutations around the HIV^{PR} active site allowing for polyprotein processing and viral maturation
406 while avoiding drug inhibition. Despite typically having poor overall viral fitness due to less
407 efficient polyprotein processing and replication relative to wildtype HIV-1 in the absence of
408 protease inhibitors, these mutant drug-resistant HIV-1 strains can persist in PLWH on antiviral
409 therapy, posing a major threat to controlling disease progression (De Luca, 2006; Martinez-
410 Picado et al., 1999; Prado et al., 2002; Resch et al., 2002). To compensate for mutations in
411 HIV^{PR} that change its substrate specificity, HIV^{gag} sometimes evolves mutations around HIV^{PR}
412 cleavage sites to permit proper polyprotein processing (Varghese et al., 2013). Here, we
413 identified multiple HIV^{PR} inhibitor-resistant strains of HIV-1 that can differentially cleave and
414 activate the CARD8 inflammasome (**Figure 4, Table S1**). As the degree of inflammation is a
415 better predictor of disease progression in untreated individuals than viral load (Deeks et al.,
416 2004; Giorgi et al., 1999), we speculate that differential CARD8 inflammasome activation could
417 influence disease progression for PLWH harboring HIV^{PR} resistance mutations that cleave
418 CARD8 more or less efficiently. More broadly, we suggest that host targets of viral proteases
419 like CARD8 may influence the selection of viral variants during treatment with antiviral protease
420 inhibitor monotherapies.

421

422 ***Viral influx activates the CARD8 inflammasome***

423 In this study, we demonstrate that HIV-dependent CARD8 inflammasome activation
424 during cell-free infection requires a cationic polymer like DEAE-dextran (**Figure 1A**). Previously,
425 we have demonstrated that CARD8 senses incoming HIV^{PR} within 2 hours post-infection, killing
426 infected cells well before $p24^{gag}$ can be expressed. Despite being infected with the same
427 amount of virus and exhibiting similar percent infection 24 hours post-infection, as measured by
428 intracellular $p24^{gag}$, with and without DEAE-dextran, we speculate that DEAE-dextran during
429 cell-free infection may increase the effective MOI or facilitate superinfection, leading to more
430 efficient viral influx to trigger CARD8 sensing, and thus $p24^{gag}$ positive cells after 24 hours may
431 be an underestimate of total infected cells in the DEAE-dextran condition. On the other hand,
432 cell-to-cell transmission of HIV-1 between infected donor cells cocultured with target cells at a
433 1:1 ratio is sufficient to induce CARD8-dependent activation in the absence of cationic polymer.
434 We infer that this is also likely a product of the efficiency of viral entry and the necessity for
435 multiple virions infecting at the same time to deliver a sufficient amount of active HIV^{PR} for
436 cytosolic CARD8 sensing. We postulate that under certain physiological conditions, cell-to-cell
437 transmission can cause CARD8 inflammasome activation when there is an influx of active
438 incoming HIV^{PR} across the viral synapse. Taken together, we speculate that both cell-free
439 infection facilitated by cationic polymer and cell-to-cell transmission can achieve sufficient levels
440 of active HIV^{PR} influx to activate the CARD8 inflammasome.

441 Macrophages have been reported to be primarily infected through phagocytosis of
442 infected CD4+ T cells or cell-to-cell transmission (Dupont and Sattentau, 2020; Martínez-
443 Méndez et al., 2017; Orenstein, 2000). We demonstrate that unlike CD4+ T cells, which are
444 rapidly depleted by HIV-1 infection and do not release IL-1β or IL-18 (Linder et al., 2020),
445 primary macrophages release pro-inflammatory cytokines in response to HIV^{PR} during cell-to-
446 cell infection (**Figure 3A, Figure 3D**), thus representing a potential source of sustained IL-1β

447 and subsequent chronic immune activation. In addition to promoting chronic immune activation,
448 HIV-dependent IL-1β release from macrophages may also contribute to HIV-1 pathogenesis by
449 activating nearby CD4+ T cells, rendering them susceptible to becoming infected with HIV-1,
450 and thus indirectly promoting CD4+ T cell depletion. Collectively with our prior work
451 (Kulsuptrakul et al., 2023), our findings provide further evidence that CARD8 inflammasome
452 activation is driven by incoming HIV^{PR} under conditions where multiple virions may enter cells,
453 and thus could be a potential driver of HIV-1 pathogenesis by promoting chronic immune
454 activation.
455

456 **METHODS**

457 ***Plasmids and Reagents***

458 pMD2.G used for $HIV\text{-}1_{LAI\text{-}VSVG}$ production was a gift from Didier Trono (Addgene). $HIV\text{-}1_{LAI}$ has
459 been previously described (Peden et al., 1991). The following reagents were obtained through
460 the NIH HIV Reagent Program, Division of AIDS, NIAID, NIH: lopinavir (LPV), nevirapine (NVP),
461 Human Immunodeficiency Virus 1 (HIV-1) NL4-3 BaL Infectious Molecular Clone (p20-36) (HIV-
462 $1_{NL4.3\text{-}BaL}$), ARP-11442, contributed by Dr. Bruce Chesebro (Chesebro et al., 1992, 1991; Toohey
463 et al., 1995; Walter et al., 2005), and Panel of Multi-Protease Inhibitor Resistant Infectious
464 Molecular Clones, HRP-12740, contributed by Dr. Robert Shafer (Varghese et al., 2013). Mutant
465 HIV^{PR} sequences were amplified from clinically-derived viral cDNA encoding protease genes
466 with resistance to multiple PRis then cloned into an NL4.3 backbone with overhangs including
467 the 3' end of gag with the gag cleavage site and the 5' end of RT as previously described
468 (Varghese et al., 2013). CARD8 variant constructs were cloned as previously described
469 (Kulsuptrakul et al., 2023). VX765 and MCC950 were sourced from Invivogen (cat: inh-vx765i-1
470 and inh-mcc, respectively).
471

472 ***Cell culture***

473 SUPT1 (ATCC) and THP-1 cells (ATCC) were cultured in RPMI (Invitrogen) with 10% FBS, 1%
474 penicillin/streptomycin antibiotics, 10 mM HEPES, 0.11 g/L sodium pyruvate, 4.5 g/L D-glucose
475 and 1% Glutamax. Primary monocytes were cultured in RPMI (Invitrogen) with 10% FBS, and
476 1% penicillin/streptomycin antibiotics and differentiated in the presence of 20ng/mL GM-CSF
477 (Peprotech cat: 300-03) and 10ng/mL M-CSF (Peprotech cat: 300-25). HEK293T (ATCC) lines
478 were cultured in DMEM (Invitrogen) with 10% FBS and 1% penicillin/streptomycin antibiotics. All
479 lines routinely tested negative for mycoplasma bacteria (Fred Hutch Specimen Processing &
480 Research Cell Bank).

481

482 ***HIV-1$_{LAI}$, HIV-1$_{LAI\text{-}VSVG}$, and HIV-1$_{NL4.3\text{-}BaL}$ production***

483 293T cells were seeded at 2-3×10^5 cells/well in six-well plates the day before transfection using
484 TransIT-LT1 reagent (Mirus Bio LLC) at 3 µL transfection reagent/well as previously described
485 (OhAinle et al., 2018). For HIV-1 production, 293Ts were transfected with 1 µg/well HIV$_{LAI}$ or
486 HIV-1$_{NL4.3\text{-}BaL}$ proviral DNA or 1 µg/well HIV$_{LAI}$ Δenv DNA and 500 ng/well pMD2.G for HIV-1$_{LAI}$,
487 HIV-1$_{NL4.3\text{-}BaL}$, and HIV-1$_{LAI\text{-}VSVG}$, respectively. One day post-transfection, media was replaced.
488 Two days post-transfection, viral supernatants were collected and filtered through a 20 µm filter
489 and aliquots were frozen at –80°C. HIV-1$_{LAI}$, HIV-1$_{NL4.3\text{-}BaL}$ and HIV-1$_{LAI\text{-}VSVG}$ proviruses were
490 previously described (Bartz and Vodicka, 1997; Gummuluru et al., 2003; Peden et al., 1991).

491

492 ***Cell-free and cell-to-cell coculture HIV-1 infection***

493 Cell-free infections with HIV-1$_{LAI\text{-}VSVG}$ were done as previously described (Kulsuptrakul et al.,
494 2023). Subsequent cell death was assessed by incubating in media containing propidium iodide
495 dye (10µg/mL) for 5 minutes at room temperature then washed once with PBS before fixing with
496 BD CytoFix/Cytoperm (cat:BDB554714) and staining for intracellular p24^{gag} (Beckman Coulter

497 cat#: 6604665) for flow cytometry. In the HIV-1 cell-to-cell transmission system, SUPT1
498 expressing CCR5 (SUPT1-CCR5) cells were spinoculated at 1100g for 30min with either HIV-
499 1_{LAI} or HIV-$1_{NL4.3\text{-}BaL}$ in the presence of 10µg/mL DEAE-dextran. SUPT1-CCR5 cells were
500 lentiviral transduced to express CCR5 (Dingens et al., 2017). After 24 hours, mock or HIV-1
501 infected SUPT1-CCR5 cells were washed three times in PBS such that DEAE-dextran and cell-
502 free virus were removed before starting coculture with THP-1 cells or MDMs. THP-1 cells and
503 MDMs were seeded at 5 x 10^5 cells/well and primed with 500ng/mL Pam3CSK4 (Invivogen) for
504 16-24 hours before coculture. Mock or infected SUPT1 cells were seeded at 5 x 10^5 cells/well.
505 Cultured supernatants from coculture were harvested 48 hours after starting the coculture for
506 the IL-1R reporter assay, which was previously described (Kulsuptrakul et al., 2023).
507

508 ***Transwell coculture HIV-1 infection***

509 SUPT1 cells were spinoculated at 1100g for 30min with HIV-1_{LAI} in the presence of 10µg/mL
510 DEAE-dextran. After 24 hours, mock or HIV-1 infected SUPT1 cells were washed 3 times in
511 PBS and either mixed in a 24-well with THP-1 cells or placed in a transwell insert above target
512 THP-1 cells at a concentration of 5 x 10^5 infected SUPT1 cells and 2.5 x 10^5 THP-1 cells per
513 well. THP-1 cells were primed overnight with 500ng/mL Pam3CSK4 before starting coculture.
514 The transwell insert has a 0.4µm membrane at the bottom of the well (ThinCert™ Tissue
515 Culture Inserts, Sterile, Greiner Bio-One cat:665640), allowing virus to pass out of the transwell
516 but not the infected cell. Reverse transcriptase activity in viral supernatants was measured
517 using the RT activity assay as previously described (Roesch et al., 2018; Vermeire et al., 2012).
518 A stock of HIV-1_{LAI} virus was titered multiple times, aliquoted at −80°C and used as the standard
519 curve in all assays.
520

521 ***Monocyte-derived macrophage isolation, differentiation, and editing***

522 Primary monocytes were isolated via negative selection using the EasySep™ Human Monocyte
523 Isolation Kit (Easy Sep, 1x10^9) (Stem Cell Technologies) according to the manufacturer's
524 protocols from PBMCs collected from healthy donors. Upon isolation, monocytes were seeded
525 at 5 x 10^5 cell/well in 24-well plates and differentiated for 5 days in the presence of media
526 containing 20ng/mL GM-CSF (Peprotech cat: 300-03) and 10ng/mL M-CSF (Peprotech cat:
527 300-25), changing media every other day. For edited MDMs, isolated monocytes were
528 electroporated in cuvettes (100µL) with 2.5-5 x 10^6 cells/nucleofection in the presence of pre-
529 complexed Cas9-RNPs (600pmol sgRNA: 100pmol Cas9) in Lonza P2 buffer using pulse code
530 DK-100. RNPs were complexed with sgRNA from the Synthego gene KO kit, which includes 3
531 sgRNAs per gene. Thus, each sgRNA was present at a 2:1 ratio with Cas9 (QB3 MacroLab). A
532 table of sgRNAs used for *AAVS1* and *CARD8* KO can be found in **Table S2** below. After
533 nucleofection, cells were supplemented with 900µL of prewarmed media and allowed to recover
534 for 30 minutes at 37°C before seeding in 48-well plates at ~6x10^5 cells/well for differentiation.
535 Media was changed 24 hours post nucleofection then differentiated for 5 more days before
536 characterizing knockout efficiency and conducting coculture experiments.

537 **Table S2:**

sgRNA	Sequence
CARD8 sgRNA1	CUCUGCAGUGACAUCAAACA
CARD8 sgRNA2	UGACGAUUGCGUUUGGUUCC
CARD8 sgRNA3	AGCGUUUGGUUCCCCACUGC
AAVS1 sgRNA 1	GUUAAUGUGGCUCUGGUUCU
AAVS1 sgRNA 2	ACCCCACAGUGGGGCCACUA
AAVS1 sgRNA 3	CCUUCCUAGUCUCCUGAUAU

538

539 ***CARD8 cleavage assay***

540 HEK293T cells were seeded at 1–1.5 × 10^5 cells/well in 24-well plates the day before
541 transfection using TransIT-LT1 reagent at 1.5 µL transfection reagent/well (Mirus Bio LLC). One
542 hundred ng of indicated constructs encoding an N-terminal mCherry-tagged CARD8 were co-

543 transfected into HEK293T cells with empty vector ('–'), HIV_{LAI} or PI-R provirus. To normalize
544 HIV^{gag} expression between $HIV\text{-}1_{LAI}$ and the PI-R clones, which are in a different vector
545 backbone, 400ng of $HIV\text{-}1_{LAI}$ and 200ng of all PI-R clones were transfected. All conditions were
546 normalized with empty vector to contain the same amount of DNA. Cytoplasmic lysates were
547 harvested 24 hours post-transfection and immunoblotted as previously described (Kulsuptrakul
548 et al., 2023).
549

550 ***HEK reconstitution assay***

551 HEK293T cells, which endogenously express CARD8, were seeded at 2.25 x 10^5 cell/well in 24-
552 well plates the day before transfection using TransIT-LT1 reagent at 1.5uL transfection
553 reagent/well (Mirus Bio LLC). Functional inflammasomes were reconstituted by transfecting in
554 5ng human CASP1 and 100ng human IL-1β. To assess the effects of different viral proteases
555 on inflammasome activation, $HIV\text{-}1_{LAI}$ or PI-R clones were co-transfected in with CASP1 and IL-
556 1β. As with the CARD8 cleavage assay, a higher amount of 250ng $HIV\text{-}1_{LAI}$ was added relative
557 to the PI-R clones, which were all added at 125ng, to normalize HIV^{gag} expression between the
558 different vector backbones. All conditions were normalized with empty vector to contain the
559 same amount of DNA. Cultured supernatant was harvested 24 hours post-transfection to assay
560 for IL-1β secretion via IL-1R reporter assay.
561

562 **Acknowledgements**

563 We thank everyone in the Emerman and Mitchell labs for helpful feedback on the project, Terry
564 Hafer and Marisa Yonemitsu for critical reading of the manuscript, Liang Shan and his lab
565 members for discussions and sharing of unpublished results and protocols, and the Fred
566 Hutchinson Shared Resources Genomics, Flow Cytometry, and Specimen Processing &
567 Research Cell Bank cores. LPV (HRP-9481), NVP (HRP-4666) and $p24^{gag}$ antibody (ARP-3537)
568 were provided by the AIDS Reagent Program, Division of AIDS, NIAID, NIH. PSM is an HHMI

569 Freeman Hrabowski Scholar and is supported by grants from the National Institutes of Health
570 (NIH) (DP2 AI 154432-01) and the Mallinckrodt Foundation to PSM. ME is supported by NIH
571 grant DP1 DA051110. JK is supported by the University of Washington Cellular and Molecular
572 Biology Training Grant (T32 GM007270).

573 **References**

574 Abela IA, Berlinger L, Schanz M, Reynell L, Günthard HF, Rusert P, Trkola A. 2012. Cell-Cell
575 Transmission Enables HIV-1 to Evade Inhibition by Potent CD4bs Directed Antibodies.
576 *PLOS Pathog* **8**:e1002634. doi:10.1371/journal.ppat.1002634
577 Agosto LM, Herring MB, Mothes W, Henderson AJ. 2018. HIV-1-Infected CD4+ T Cells
578 Facilitate Latent Infection of Resting CD4+ T Cells through Cell-Cell Contact. *Cell Rep*
579 **24**:2088–2100. doi:10.1016/j.celrep.2018.07.079
580 Agosto LM, Uchil PD, Mothes W. 2015. HIV cell-to-cell transmission: effects on pathogenesis
581 and antiretroviral therapy. *Trends Microbiol* **23**:289–295. doi:10.1016/j.tim.2015.02.003
582 Bailey CA, Miller DK, Lenard J. 1984. Effects of DEAE-dextran on infection and hemolysis by
583 VSV. Evidence that nonspecific electrostatic interactions mediate effective binding of
584 VSV to cells. *Virology* **133**:111–118. doi:10.1016/0042-6822(84)90429-x
585 Bartz SR, Vodicka MA. 1997. Production of High-Titer Human Immunodeficiency Virus Type 1
586 Pseudotyped with Vesicular Stomatitis Virus Glycoprotein. *Methods* **12**:337–342.
587 doi:10.1006/meth.1997.0487
588 Baxter AE, Russell RA, Duncan CJA, Moore MD, Willberg CB, Pablos JL, Finzi A, Kaufmann
589 DE, Ochsenbauer C, Kappes JC, Groot F, Sattentau QJ. 2014. Macrophage infection via
590 selective capture of HIV-1-infected CD4+ T cells. *Cell Host Microbe* **16**:711–721.
591 doi:10.1016/j.chom.2014.10.010
592 Brenchley JM, Paiardini M, Knox KS, Asher AI, Cervasi B, Asher TE, Scheinberg P, Price DA,
593 Hage CA, Kholi LM, Khoruts A, Frank I, Else J, Schacker T, Silvestri G, Douek DC.
594 2008. Differential Th17 CD4 T-cell depletion in pathogenic and nonpathogenic lentiviral
595 infections. *Blood* **112**:2826–2835. doi:10.1182/blood-2008-05-159301
596 Brenchley JM, Price DA, Schacker TW, Asher TE, Silvestri G, Rao S, Kazzaz Z, Bornstein E,
597 Lambotte O, Altmann D, Blazar BR, Rodriguez B, Teixeira-Johnson L, Landay A, Martin
598 JN, Hecht FM, Picker LJ, Lederman MM, Deeks SG, Douek DC. 2006. Microbial
599 translocation is a cause of systemic immune activation in chronic HIV infection. *Nat Med*
600 **12**:1365–1371. doi:10.1038/nm1511
601 Broz P, Dixit VM. 2016. Inflammasomes: mechanism of assembly, regulation and signalling. *Nat*
602 *Rev Immunol* **16**:407–420. doi:10.1038/nri.2016.58
603 Castro LK, Daugherty MD. 2023. Tripping the wire: sensing of viral protease activity by CARD8
604 and NLRP1 inflammasomes. *Curr Opin Immunol* **83**:102354.
605 doi:10.1016/j.coi.2023.102354
606 Chen P, Hübner W, Spinelli MA, Chen BK. 2007. Predominant mode of human
607 immunodeficiency virus transfer between T cells is mediated by sustained Env-
608 dependent neutralization-resistant virological synapses. *J Virol* **81**:12582–12595.
609 doi:10.1128/JVI.00381-07
610 Chesebro B, Nishio J, Perryman S, Cann A, O'Brien W, Chen IS, Wehrly K. 1991. Identification
611 of human immunodeficiency virus envelope gene sequences influencing viral entry into
612 CD4-positive HeLa cells, T-leukemia cells, and macrophages. *J Virol* **65**:5782–5789.
613 doi:10.1128/JVI.65.11.5782-5789.1991

614 Chesebro B, Wehrly K, Nishio J, Perryman S. 1992. Macrophage-tropic human
615 immunodeficiency virus isolates from different patients exhibit unusual V3 envelope
616 sequence homogeneity in comparison with T-cell-tropic isolates: definition of critical
617 amino acids involved in cell tropism. *J Virol* **66**:6547–6554. doi:10.1128/JVI.66.11.6547-
618 6554.1992
619 Chun T-W, Carruth L, Finzi D, Shen X, DiGiuseppe JA, Taylor H, Hermankova M, Chadwick K,
620 Margolick J, Quinn TC, Kuo Y-H, Brookmeyer R, Zeiger MA, Barditch-Crovo P, Siliciano
621 RF. 1997a. Quantification of latent tissue reservoirs and total body viral load in HIV-1
622 infection. *Nature* **387**:183–188. doi:10.1038/387183a0
623 Chun T-W, Finzi D, Margolick J, Chadwick K, Schwartz D, Siliciano RF. 1995. In vivo fate of
624 HIV-1-infected T cells: Quantitative analysis of the transition to stable latency. *Nat Med*
625 **1**:1284–1290. doi:10.1038/nm1295-1284
626 Chun T-W, Stuyver L, Mizell SB, Ehler LA, Mican JAM, Baseler M, Lloyd AL, Nowak MA, Fauci
627 AS. 1997b. Presence of an inducible HIV-1 latent reservoir during highly active
628 antiretroviral therapy. *Proc Natl Acad Sci* **94**:13193–13197.
629 doi:10.1073/pnas.94.24.13193
630 Clark KM, Kim JG, Wang Q, Gao H, Presti RM, Shan L. 2022. Chemical inhibition of DPP9
631 sensitizes the CARD8 inflammasome in HIV-1-infected cells. *Nat Chem Biol* 1–9.
632 doi:10.1038/s41589-022-01182-5
633 Coll RC, Robertson AAB, Chae JJ, Higgins SC, Muñoz-Planillo R, Inserra MC, Vetter I, Dungan
634 LS, Monks BG, Stutz A, Croker DE, Butler MS, Haneklaus M, Sutton CE, Núñez G, Latz
635 E, Kastner DL, Mills KHG, Masters SL, Schroder K, Cooper MA, O'Neill LAJ. 2015. A
636 small-molecule inhibitor of the NLRP3 inflammasome for the treatment of inflammatory
637 diseases. *Nat Med* **21**:248–255. doi:10.1038/nm.3806
638 Collman R, Godfrey B, Cutilli J, Rhodes A, Hassan NF, Sweet R, Douglas SD, Friedman H,
639 Nathanson N, Gonzalez-Scarano F. 1990. Macrophage-tropic strains of human
640 immunodeficiency virus type 1 utilize the CD4 receptor. *J Virol* **64**:4468–4476.
641 doi:10.1128/jvi.64.9.4468-4476.1990
642 Collman R, Hassan NF, Walker R, Godfrey B, Cutilli J, Hastings JC, Friedman H, Douglas SD,
643 Nathanson N. 1989. Infection of monocyte-derived macrophages with human
644 immunodeficiency virus type 1 (HIV-1). Monocyte-tropic and lymphocyte-tropic strains of
645 HIV-1 show distinctive patterns of replication in a panel of cell types. *J Exp Med*
646 **170**:1149–1163. doi:10.1084/jem.170.4.1149
647 Conant D, Hsiau T, Rossi N, Oki J, Maures T, Waite K, Yang J, Joshi S, Kelso R, Holden K,
648 Enzmann BL, Stoner R. 2022. Inference of CRISPR Edits from Sanger Trace Data.
649 *CRISPR J* **5**:123–130. doi:10.1089/crispr.2021.0113
650 De Luca A. 2006. The impact of resistance on viral fitness and its clinical implications In: Geretti
651 AM, editor. Antiretroviral Resistance in Clinical Practice. London: Mediscript.
652 Deeks SG, Kitchen CMR, Liu L, Guo H, Gascon R, Narváez AB, Hunt P, Martin JN, Kahn JO,
653 Levy J, McGrath MS, Hecht FM. 2004. Immune activation set point during early HIV
654 infection predicts subsequent CD4+ T-cell changes independent of viral load. *Blood*
655 **104**:942–947. doi:10.1182/blood-2003-09-3333
656 Del Portillo A, Tripodi J, Najfeld V, Wodarz D, Levy DN, Chen BK. 2011. Multiploid Inheritance
657 of HIV-1 during Cell-to-Cell Infection ▿. *J Virol* **85**:7169–7176. doi:10.1128/JVI.00231-11
658 Dingens AS, Haddox HK, Overbaugh J, Bloom JD. 2017. Comprehensive mapping of HIV-1
659 escape from a broadly neutralizing antibody. *Cell Host Microbe* **21**:777-787.e4.
660 doi:10.1016/j.chom.2017.05.003
661 Doitsh G, Galloway NL, Geng X, Yang Z, Monroe KM, Zepeda O, Hunt PW, Hatano H, Sowinski
662 S, Muñoz-Arias I, Greene WC. 2014. Pyroptosis drives CD4 T-cell depletion in HIV-1
663 infection. *Nature* **505**:509–514. doi:10.1038/nature12940

664 Dufloo J, Bruel T, Schwartz O. 2018. HIV-1 cell-to-cell transmission and broadly neutralizing
665 antibodies. *Retrovirology* **15**:51. doi:10.1186/s12977-018-0434-1
666 Duncan CJA, Russell RA, Sattentau QJ. 2013. High multiplicity HIV-1 cell-to-cell transmission
667 from macrophages to CD4+ T cells limits antiretroviral efficacy. *AIDS* **27**:2201.
668 doi:10.1097/QAD.0b013e3283632ec4
669 Dupont M, Sattentau QJ. 2020. Macrophage Cell-Cell Interactions Promoting HIV-1 Infection.
670 *Viruses* **12**:492. doi:10.3390/v12050492
671 Fink SL, Cookson BT. 2005. Apoptosis, Pyroptosis, and Necrosis: Mechanistic Description of
672 Dead and Dying Eukaryotic Cells. *Infect Immun* **73**:1907–1916.
673 doi:10.1128/IAI.73.4.1907-1916.2005
674 Galloway NLK, Doitsh G, Monroe KM, Yang Z, Muñoz-Arias I, Levy DN, Greene WC. 2015.
675 Cell-to-Cell Transmission of HIV-1 Is Required to Trigger Pyroptotic Death of Lymphoid-
676 Tissue-Derived CD4 T Cells. *Cell Rep* **12**:1555–1563. doi:10.1016/j.celrep.2015.08.011
677 Giorgi JV, Hultin LE, McKeating JA, Johnson TD, Owens B, Jacobson LP, Shih R, Lewis J,
678 Wiley DJ, Phair JP, Wolinsky SM, Detels R. 1999. Shorter Survival in Advanced Human
679 Immunodeficiency Virus Type 1 Infection Is More Closely Associated with T Lymphocyte
680 Activation than with Plasma Virus Burden or Virus Chemokine Coreceptor Usage. *J*
681 *Infect Dis* **179**:859–870. doi:10.1086/314660
682 Gosselin A, Monteiro P, Chomont N, Diaz-Griffero F, Said EA, Fonseca S, Wacleche V, El-Far
683 M, Boulassel M-R, Routy J-P, Sekaly R-P, Ancuta P. 2009. Peripheral Blood
684 CCR4+CCR6+ and CXCR3+CCR6+ CD4+ T Cells Are Highly Permissive to HIV-1
685 Infection. *J Immunol* **184**:1604–1616. doi:10.4049/jimmunol.0903058
686 Gummuluru S, Rogel M, Stamatatos L, Emerman M. 2003. Binding of Human Immunodeficiency
687 Virus Type 1 to Immature Dendritic Cells Can Occur Independently of DC-SIGN and
688 Mannose Binding C-Type Lectin Receptors via a Cholesterol-Dependent Pathway. *J*
689 *Virol* **77**:12865–12874. doi:10.1128/JVI.77.23.12865-12874.2003
690 Hornung V, Ablasser A, Charrel-Dennis M, Bauernfeind F, Horvath G, Caffrey DR, Latz E,
691 Fitzgerald KA. 2009. AIM2 recognizes cytosolic dsDNA and forms a caspase-1
692 activating inflammasome with ASC. *Nature* **458**:514–518. doi:10.1038/nature07725
693 Iwami S, Takeuchi JS, Nakaoka S, Mammano F, Clavel F, Inaba H, Kobayashi T, Misawa N,
694 Aihara K, Koyanagi Y, Sato K. 2015. Cell-to-cell infection by HIV contributes over half of
695 virus infection. *eLife* **4**:e08150. doi:10.7554/eLife.08150
696 Jiang Z, Wei F, Zhang Y, Wang T, Gao W, Yu S, Sun H, Pu J, Sun Y, Wang M, Tong Q, Gao C,
697 Chang K-C, Liu J. 2021. IFI16 directly senses viral RNA and enhances RIG-I
698 transcription and activation to restrict influenza virus infection. *Nat Microbiol* **6**:932–945.
699 doi:10.1038/s41564-021-00907-x
700 Jolly C, Booth NJ, Neil SJD. 2010. Cell-Cell Spread of Human Immunodeficiency Virus Type 1
701 Overcomes Tetherin/BST-2-Mediated Restriction in T cells. *J Virol* **84**:12185–12199.
702 doi:10.1128/jvi.01447-10
703 Kulsuptrakul J, Turcotte EA, Emerman M, Mitchell PS. 2023. A human-specific motif facilitates
704 CARD8 inflammasome activation after HIV-1 infection. *eLife* **12**:e84108.
705 doi:10.7554/eLife.84108
706 Linder A, Bauernfried S, Cheng Y, Albanese M, Jung C, Keppler OT, Hornung V. 2020. CARD8
707 inflammasome activation triggers pyroptosis in human T cells. *EMBO J* **39**:e105071.
708 doi:10.15252/embj.2020105071
709 Lopez P, Koh WH, Hnatiuk R, Murooka TT. 2019. HIV Infection Stabilizes Macrophage-T Cell
710 Interactions To Promote Cell-Cell HIV Spread. *J Virol* **93**:e00805-19.
711 doi:10.1128/JVI.00805-19
712 Martin N, Welsch S, Jolly C, Briggs JAG, Vaux D, Sattentau QJ. 2010. Virological Synapse-
713 Mediated Spread of Human Immunodeficiency Virus Type 1 between T Cells Is
714 Sensitive to Entry Inhibition. *J Virol* **84**:3516–3527. doi:10.1128/jvi.02651-09

715 Martínez-Méndez D, Rivera-Toledo E, Ortega E, Licona-Limón I, Huerta L. 2017. Monocyte-
716 lymphocyte fusion induced by the HIV-1 envelope generates functional heterokaryons
717 with an activated monocyte-like phenotype. *Exp Cell Res* **352**:9–19.
718 doi:10.1016/j.yexcr.2017.01.014
719 Martinez-Picado J, Savara AV, Sutton L, D'Aquila RT. 1999. Replicative fitness of protease
720 inhibitor-resistant mutants of human immunodeficiency virus type 1. *J Virol* **73**:3744–
721 3752. doi:10.1128/JVI.73.5.3744-3752.1999
722 Monroe KM, Yang Z, Johnson JR, Geng X, Doitsh G, Krogan NJ, Greene WC. 2014. IFI16 DNA
723 Sensor Is Required for Death of Lymphoid CD4 T-cells Abortively Infected with HIV.
724 *Science* **343**:428–432. doi:10.1126/science.1243640
725 Nadkarni R, Chu WC, Lee CQE, Mohamud Y, Yap L, Toh GA, Beh S, Lim R, Fan YM, Zhang
726 YL, Robinson K, Tryggvason K, Luo H, Zhong F, Ho L. 2022. Viral proteases activate the
727 CARD8 inflammasome in the human cardiovascular system. *J Exp Med* **219**:e20212117.
728 doi:10.1084/jem.20212117
729 OhAinle M, Helms L, Vermeire J, Roesch F, Humes D, Basom R, Delrow JJ, Overbaugh J,
730 Emerman M. 2018. A virus-packageable CRISPR screen identifies host factors
731 mediating interferon inhibition of HIV. *eLife* **7**:e39823. doi:10.7554/eLife.39823
732 Orenstein JM. 2000. In Vivo Cytolysis and Fusion of Human Immunodeficiency Virus Type 1-
733 Infected Lymphocytes in Lymphoid Tissue. *J Infect Dis* **182**:338–342.
734 doi:10.1086/315640
735 Peden K, Emerman M, Montagnier L. 1991. Changes in growth properties on passage in tissue
736 culture of viruses derived from infectious molecular clones of HIV-1LAI, HIV-1MAL, and
737 HIV-1ELI. *Virology* **185**:661–672. doi:10.1016/0042-6822(91)90537-L
738 Prado JG, Wrin T, Beauchaine J, Ruiz L, Petropoulos CJ, Frost SDW, Clotet B, D'Aquila RT,
739 Martinez-Picado J. 2002. Amprenavir-resistant HIV-1 exhibits lopinavir cross-resistance
740 and reduced replication capacity. *AIDS Lond Engl* **16**:1009–1017.
741 doi:10.1097/00002030-200205030-00007
742 Primiano MJ, Lefker BA, Bowman MR, Bree AG, Hubeau C, Bonin PD, Mangan M, Dower K,
743 Monks BG, Cushing L, Wang S, Guzova J, Jiao A, Lin L-L, Latz E, Hepworth D, Hall JP.
744 2016. Efficacy and Pharmacology of the NLRP3 Inflammasome Inhibitor CP-456,773
745 (CRID3) in Murine Models of Dermal and Pulmonary Inflammation. *J Immunol*
746 **197**:2421–2433. doi:10.4049/jimmunol.1600035
747 Resch W, Ziermann R, Parkin N, Gamarnik A, Swanstrom R. 2002. Nelfinavir-resistant,
748 amprenavir-hypersusceptible strains of human immunodeficiency virus type 1 carrying
749 an N88S mutation in protease have reduced infectivity, reduced replication capacity, and
750 reduced fitness and process the Gag polyprotein precursor aberrantly. *J Virol* **76**:8659–
751 8666. doi:10.1128/jvi.76.17.8659-8666.2002
752 Richardson MW, Carroll RG, Stremlau M, Korokhov N, Humeau LM, Silvestri G, Sodroski J,
753 Riley JL. 2008. Mode of Transmission Affects the Sensitivity of Human
754 Immunodeficiency Virus Type 1 to Restriction by Rhesus TRIM5α. *J Virol* **82**:11117–
755 11128. doi:10.1128/jvi.01046-08
756 Rodriguez-Garcia M, Barr FD, Crist SG, Fahey JV, Wira CR. 2014. Phenotype and susceptibility
757 to HIV infection of CD4+ Th17 cells in the human female reproductive tract. *Mucosal*
758 *Immunol* **7**:1375–1385. doi:10.1038/mi.2014.26
759 Roesch F, OhAinle M, Emerman M. 2018. A CRISPR screen for factors regulating SAMHD1
760 degradation identifies IFITMs as potent inhibitors of lentiviral particle delivery.
761 *Retrovirology* **15**:26. doi:10.1186/s12977-018-0409-2
762 Russell RA, Martin N, Mitar I, Jones E, Sattentau QJ. 2013. Multiple proviral integration events
763 after virological synapse-mediated HIV-1 spread. *Virology* **443**:143–149.
764 doi:10.1016/j.virol.2013.05.005

765 Stanford - HIV Drug Resistance Database. n.d. https://hivdb.stanford.edu/page/release-
766 notes/#consensusbsequences
767 Thompson MR, Sharma S, Atianand M, Jensen SB, Carpenter S, Knipe DM, Fitzgerald KA,
768 Kurt-Jones EA. 2014. Interferon γ-inducible Protein (IFI) 16 Transcriptionally Regulates
769 Type I Interferons and Other Interferon-stimulated Genes and Controls the Interferon
770 Response to both DNA and RNA Viruses. *J Biol Chem* **289**:23568–23581.
771 doi:10.1074/jbc.M114.554147
772 Toohey K, Wehrly K, Nishio J, Perryman S, Chesebro B. 1995. Human immunodeficiency virus
773 envelope V1 and V2 regions influence replication efficiency in macrophages by affecting
774 virus spread. *Virology* **213**:70–79. doi:10.1006/viro.1995.1547
775 Tsu BV, Agarwal R, Gokhale NS, Kulsuptrakul J, Ryan AP, Fay EJ, Castro LK, Beierschmitt C,
776 Yap C, Turcotte EA, Delgado-Rodriguez SE, Vance RE, Hyde JL, Savan R, Mitchell PS,
777 Daugherty MD. 2023. Host-specific sensing of coronaviruses and picornaviruses by the
778 CARD8 inflammasome. *PLOS Biol* **21**:e3002144. doi:10.1371/journal.pbio.3002144
779 Varghese V, Mitsuya Y, Fessel WJ, Liu TF, Melikian GL, Katzenstein DA, Schiffer CA, Holmes
780 SP, Shafer RW. 2013. Prototypical Recombinant Multi-Protease-Inhibitor-Resistant
781 Infectious Molecular Clones of Human Immunodeficiency Virus Type 1. *Antimicrob*
782 *Agents Chemother* **57**:4290–4299. doi:10.1128/AAC.00614-13
783 Vermeire J, Naessens E, Vanderstraeten H, Landi A, Iannucci V, Van Nuffel A, Taghon T,
784 Pizzato M, Verhasselt B. 2012. Quantification of reverse transcriptase activity by real-
785 time PCR as a fast and accurate method for titration of HIV, lenti- and retroviral vectors.
786 *PloS One* **7**:e50859. doi:10.1371/journal.pone.0050859
787 Walter BL, Wehrly K, Swanstrom R, Platt E, Kabat D, Chesebro B. 2005. Role of low CD4 levels
788 in the influence of human immunodeficiency virus type 1 envelope V1 and V2 regions on
789 entry and spread in macrophages. *J Virol* **79**:4828–4837. doi:10.1128/JVI.79.8.4828-
790 4837.2005
791 Wang Q, Clark KM, Tiwari R, Raju N, Tharp GK, Rogers J, Harris RA, Raveendran M, Bosinger
792 SE, Burdo TH, Silvestri G, Shan L. 2024. The CARD8 inflammasome dictates HIV/SIV
793 pathogenesis and disease progression. *Cell* **187**:1223-1237.e16.
794 doi:10.1016/j.cell.2024.01.048
795 Wang Q, Gao H, Clark KM, Mugisha CS, Davis K, Tang JP, Harlan GH, DeSelm CJ, Presti RM,
796 Kutluay SB, Shan L. 2021. CARD8 is an inflammasome sensor for HIV-1 protease
797 activity. *Science* **371**:eabe1707. doi:10.1126/science.abe1707
798 Wannamaker W, Davies R, Namchuk M, Pollard J, Ford P, Ku G, Decker C, Charifson P, Weber
799 P, Germann UA, Kuida K, Randle JCR. 2007. (S)-1-((S)-2-{[1-(4-amino-3-chloro-phenyl)-
800 methanoyl]-amino}-3,3-dimethyl-butanoyl)-pyrrolidine-2-carboxylic acid ((2R,3S)-2-
801 ethoxy-5-oxo-tetrahydro-furan-3-yl)-amide (VX-765), an orally available selective
802 interleukin (IL)-converting enzyme/caspase-1 inhibitor, exhibits potent anti-inflammatory
803 activities by inhibiting the release of IL-1beta and IL-18. *J Pharmacol Exp Ther* **321**:509–
804 516. doi:10.1124/jpet.106.111344
805 Xie M, Leroy H, Mascarau R, Woottum M, Dupont M, Ciccone C, Schmitt A, Raynaud-Messina
806 B, Vérollet C, Bouchet J, Bracq L, Benichou S. 2019. Cell-to-Cell Spreading of HIV-1 in
807 Myeloid Target Cells Escapes SAMHD1 Restriction. *mBio* **10**:10.1128/mbio.02457-19.
808 doi:10.1128/mbio.02457-19
809 Zhang C, Song J-W, Huang H-H, Fan X, Huang L, Deng J-N, Tu B, Wang K, Li J, Zhou M-J,
810 Yang C-X, Zhao Q-W, Yang T, Wang L-F, Zhang J-Y, Xu R-N, Jiao Y-M, Shi M, Shao F,
811 Sékaly R-P, Wang F-S. 2021. NLRP3 inflammasome induces $CD4^+$ T cell loss in
812 chronically HIV-1–infected patients. *J Clin Invest* **131**. doi:10.1172/JCI138861
813 Zhong P, Agosto LM, Ilinskaya A, Dorjbal B, Truong R, Derse D, Uchil PD, Heidecker G, Mothes
814 W. 2013. Cell-to-Cell Transmission Can Overcome Multiple Donor and Target Cell

815 Barriers Imposed on Cell-Free HIV. *PLOS ONE* **8**:e53138.
816 doi:10.1371/journal.pone.0053138
817